Research Inventy: International Journal of Engineering And Science
Vol.10, Issue 10 (October 2020), PP 20-30
Issn (e): 2278-4721, Issn (p):2319-6483, www.researchinventy.com

Synthesis and AB INTIO Structure Determination Of Mixed Valence a Novel Ternary Oxide $Cd_{0.54}$ $La_{2.5}$ $Pb_{1.25}$ $N_{0.21}$ $O_{0.25}$ and Study the Physical Properties

Yuv Raj Sahu, Rohit K. Dev, Kalpana Mishra and Parashuram Mishra*,
Bioinorganic and Materials Chemistry Research Laboratory,
Tribhuvan University, M. M. A. M. Campus, Biratnagar, Nepal

Abstract: *Powder X-ray diffraction (XRD) has been exploited to establish the structural properties of a porous inter-penetrated metal framework material prepared by solid-state grinding, recognizing that product phases from mechano-chemical synthesis are typically microcrystalline powders. The importance of subjecting the powder XRD data to rigorous scrutiny in such applications is emphasized. The present work deals with the ab initio structure determination of the heavy metal framework having mixed valence in $Cd_{0.54}$ $La_{2.5}$ $Pb_{1.25}$ $N_{0.21}$ $O_{0.25}$ from precession electron diffraction intensities. The metal framework of the compound was solved in this investigation via direct methods from* ***hk0*** *precession electron diffraction intensities recorded with a Philips EM400 at 100 kV. A subsequent (kinematical) least-squares refinement with electron intensities yielded slightly improved co-ordinates for the 11 heavy atoms in the structure. Chemical analysis of several crystallites by EDX is in agreement with the formula $Cd_{0.54}$ $La_{2.5}$ $Pb_{1.25}$ $N_{0.21}$ $O_{0.25}$ Moreover, the structure was independently determined by Rietveld refinement from X-ray powder data obtained from a multi-phasic sample. The compound crystallizes in the triclinic crystal system space group P-1 with refined lattice parameters of $Cd_{0.54}$ $La_{2.5}$ $Pb_{1.25}$ $N_{0.21}$ $O_{0.25}$ are and refine values Rp=0.2501,Rwp=0.3065 and GOF=0.0135.*

Keywords: *Crystal, structure triclinic, investigation, multiphase, independent*

Date of Submission: 01-10-2020 Date of Acceptance: 14-10-2020

I. INTRODUCTION

Metal oxides contain mixed valence are very useful for ordering molecules intolamelar structure. These compounds are hybrid inorganic and organic by nature materials and usually consist of alternating inorganic layers. They can be prepared as polycrystalline solids, thin films or membranes depending upon applications. Nowadays, there is a great deal of work in metal oxide contained mixed valence due to interesting physical and chemical properties. Recent investigation of structural and conductivity properties of Cd0.775¸n 0.225O1.5 oxide conductors (¸n"La, Pr, Nd, Sm, Eu, Gd, Tb, Dy), which belong to the dimorphic rhombohedra Bi}Sr}O structural-type family, has proved a close conductivity}composition dependence (Thomas E Weiricha, et al, 2006). This has been interpreted on the basis of structural data obtained from Rietveld structure refinements based on previous crystal structure investigations (Zhengyang Zhou et al., 2019). The structure is built from cationic slabs parallel to (001) faces of the hexagonal cells. There are nine formula units La0.775¸ n0. 225O1.5 per triclinic cell, distributed over three slabs. Each slab is constituted from a mixed Lai3`/¸n3` layer, sandwiched between two La3+` layers, and two oxygen sites are located inside; complementary oxide ions, implied by the formulation stoichiometry, are distributed over one or two sites of the interslab space and exhibit a high mobility, mainly responsible for the conductivity . Depending on the rare-earth nature, a b1 high-temperature form is observed, with a closely hexagonal related structure; its formation from the b2 low-temperature variety occurs during a phase transition that has been attributed to a cationic disordering in the mixed Bi3`/¸n3` layers. It is accompanied by sudden increases of both lattice parameters, of oxide occupancy in inter slab spaces, and of the conductivity. The pure iron oxide conductor character of the b1 variety has been clearly demonstrated for the alkaline-earth-based solid solutions (Krichen et al., 2020) and has been also verified for lanthanides-based solid solutions. The pure iron oxide conductor character of the b1 variety has been clearly demonstrated for the alkaline-earth-based solid solutions and has been also verified for vanadium -based solid. The thickness of the cationic slabs, which is the largest for the vanadium term oxide $Cd_{0.54}$ $La_{2.5}$ $Pb_{1.25}$ $N_{0.21}$ $O_{0.25}$ (the best oxide conductor ever evidenced in this family: at 400^0C is 10^{-3} Scm~1 with E 0.8 eV), appears to be an important factor for these attractive conductivity properties. $Cd_{0.54}$ $La_{2.5}$ $Pb_{1.25}$ $N_{0.21}$ $O_{0.25}$ is a term of a wide solid solution

domain. The crystal structure of $Bi_{1.25}$ $V_{0.123}$ Ca $_{0.245}$ has been determined from powder diffraction data using a combination of direct methods and the novel approach of applying simulated annealing methods simultaneously to X-ray powder pattern by ab initio method. $Cd_{0.54}$ $La_{2.5}$ $Pb_{1.25}$ $N_{0.21}$ O $_{0.25}$ is a polar, non-centro-symmetric, second harmonic generation active material and its crystal structure is one of the more complex to be solved ab initio from powder diffraction data. Many of the important heterogeneous catalysts are transition and non-transition metals dispersed on oxide supports. Although the primary function of the support is to increase the surface area of the metal, there is now a vast literature documenting that supports can cause pronounced changes in the catalytic and chemisorptions properties of the metal (Kanth and Mishra, 2020). In particular, when group 8-10 metals are dispersed on reducible ions supports such as oxide of metal ions. The chemisorptions properties and activity of the catalyst depend on the reduction temperature used for pretreatment. Numerous mechanisms have been proposed to account for this suppression of chemisorptions and the associated change in catalytic activity; the most popular is the diffusion of reduced oxide $Cd_{0.54}$ $La_{2.5}$ $Pb_{1.25}$ $N_{0.21}$ O $_{0.25}$ moieties onto the metal, thereby blocking metal sites. However, numerous experimental observations are left unexplained by this model. For example, changes in the magnetic properties of Cd/ La, composites with reduction temperature indicate that the Bi does not remain as elemental bismuth, but forms a Cd-La- Pb multiphase phase. Unfortunately, investigations into the role of compound formation in producing the observed effect have been hindered by the fact that relatively few ternary oxides containing both an early and a late transition and non-transition metal contained mixed valence are known.. It is interesting to note that superconductivity has been observed in some of the ternary oxide phases having the Bi and V structure type and for $Cd_{0.54}$ $La_{2.5}$ $Pb_{1.25}$ $N_{0.21}$ O $_{0.25}$ In this paper, we report the synthesis and crystal structure of $Cd_{0.54}$ $La_{2.5}$ $Pb_{1.25}$ $N_{0.21}$ O $_{0.25}$ by ab initio method via powder XRD and also study the morphology and electrical property.

EXPERIMENTAL PROCEDURE

2.1Material and Methods

All chemicals used were analytical grade purchase from Sigma Aldrich U. S. A.. A polycrystalline sample of $Cd_{0.54}$ $La_{2.5}$ $Pb_{1.25}$ $N_{0.21}$ O $_{0.25}$ was synthesized by a standard solid state reaction using a mixture of high purity reagents of La2(CO)3−Pb(NO3)3 and $CdCO_3$ as the starting materials in the molar ratio of 1 : 1 : 2. The mixture was ground carefully, homogenized thoroughly with methanol (99%) in an agate mortar and then packed into an alumina crucible and calcined at 1000°C in air for 10h with several intermediate grindings [4]. Finally the product was pressed into pallets and sintered at 100 K/h. Powder X-ray diffraction (XRD) data were collected at room temperature in the angular range of 2 θ =10 to 90 with scan step width of 0.02° and a fixed containing time of 15 s using Philips powder diffractometer with graphite monochromatic CuKa radiation. The powder was rotated during the data collection to minimize preferred Orientation effect if any. The program TREOR in CRYSFIRE was used to index the powder pattern which give orthorhombic cell system.SIRPOW92 was used to locate the positional parameters of constituent atoms. The full pattern is fitting and peak decomposition in the space group P n -3 n (222 using check cell program). The structural parameters were refined by the Rietveld method using the JANA program which gave Rp=0.2501, Rwp=0.3065 and GOF=0.0135. The density is determined by Archimedes principle. The morphology of titled compound was determined using SEM. For the electrical studies, the measurements were preceded by a pretreatment of the sample in order to reduce the mean particle size of the obtained powder. After these treatments, the sample achieved about 85% of the theoretical density with the final diameter of 6 mm and thickness of 23mm. The relative density of the sample before the mechanical grinding was 79 %. Platinum electrodes were connected to the two faces of the pellet via a platinum paste to keep good electric contacts. Impedance spectroscopy measurements were carried out by using a Hewlett-Packard 4192a Impedance Analyzer. The impedance spectra were recorded in the 5 Hz-13 MHz frequency range. Electrical conductivity measurements of representative $Cd_{0.54}$ $La_{2.5}$ $Pb_{1.25}$ $N_{0.21}$ O $_{0.25}$ were carried out by complex impedance spectroscopy with a 1174 Solartron frequency response analyzer coupled to a 1266 Solartron electrochemical interface. Pellets of about 14 mm diameter and 1 mm thickness were prepared by cold pressing of a mechanically activated powder mixture with the composition: $Cd_{0.54}$ $La_{2.5}$ $Pb_{1.25}$ $N_{0.21}$ O $_{0.25}$ .To form the phase, the pellets were heated at 7003C during 12 h and slowly cooled to room temperature. This synthesis method was employed to improve the ceramic quality, as it has been shown for other materials (J You et al., 2018). The formed phases and crystallinity were studied by X-ray powder diffraction. Platinum electrodes were deposited on the two faces by sputtering, and measurements were carried out in the temperature range 200-650^{0}C, at steady temperatures, with pellets under air flow and the frequency range was fixed (Y. Liang et al., 2007).

2.2Physical Measurements

X-ray powder diffraction data were obtained on a Philips powder diffractometer using Bragg Brentano geometry, with a back monochromatic CuKa radiation having 1.5456(A) wavelength. Diffraction spectra were

scanned by steps of 0.023 (2h) over the angle range 5-50 (2θ), with a counting time of 1.5 s per step. Each sample was rotated 3.14 radian s^{-1} during the data recording, in order to minimize the orientation effects resulting from the material compaction (P. Mishra, 2011). The pattern peak positions are extracted with the Topas P of Bruker-Diffrac1- 64 software package, where each peak profile is refined using the pseudo-Voigt function. The accurate cell parameters of the different samples were refined from 5 to 50 reflections cubic. The crystal structure determination of the phase was carried out for the Philips powder diffractometer $Cd_{0.54}$ $La_{2.5}$ $Pb_{1.25}$ $N_{0.21}$ $O_{0.25}$ parent composition. The first attempts were undertaken by recording X-ray diffraction data, but each time, the intensities diffraction pattern was erroneous by the preferential orientation phenomenon. To minimize the preferential orientation effect and indeed be able to separate the oxygen and N atoms of the heavy atoms Bi and V at room temperature. The crystal structure determination has been concluded by using alternately the **JANA -16** and **EXPO -7** programs. Dilatometric and conductivity investigations were made on samples pelletized at room temperature (diameter 5 mm, thickness approx. 3 mm), then sintered at 900^0C for 15 h and quenched to room temperature, in liquid nitrogen. The degree of compactness in all cases ranged between 75 and 92%.Dilatometric studies were performed on a Linseis L75 dilatometer with a heating rate of 0.43C/min between 20 and 700^0C. For conductivity measurements, gold electrodes were vacuum deposited on both #at surfaces of the pellets using the sputtering method. The measurements were obtained by impedance spectrometry in the frequency range 1-106 Hz, using a frequency response analyzer Schlumberger 1170; for a given temperature, each set of values was recorded after a 1h stabilization time. The density was calculated by Archimedes principle.

III. RESULTS AND DISCUSSIONS

The extensive search for novel inorganic materials with open frameworks formed of tetrahedral and octahedral delimiting inter-layer spaces (2D), tunnels (3D) or cages (1D) where cations are housed, represent currently a field of intense activity including several disciplines: solid-state chemistry, physics, mechanics, and mainly ionic conductivity properties and their use as battery materials oxides of metals and alkaline cations are well known for their thermal stability and the simplicity of syntheses , which is important for many practical applications lithium batteries (P. Bertocco, et al. 2019). The compound was prepared from Bi_2O_3−NH_4VO_3 and $CaCO_3$ as starting material oxides. Calcium oxide powder was dried and decarbonated at 1000 ^{0}C over night prior to use. The oxides were weighed in stoichiometric proportions and ground together in an agate mortar. The prepared composition was heated upto1400 ^{0}C for overnight in an alumina crucible, no particular condition was used in order to cool down the samples (Mah Jebli et al.,2019).This procedure was applied at least twice in order to establish compound as verified by X-ray powder diffraction. The final compound is white in colour.

3.1. Crystal structure of $Cd_{0.54}$ $La_{2.5}$ $Pb_{1.25}$ $N_{0.21}$ $O_{0.25}$

The framework structure of $Cd_{0.54}$ $La_{2.5}$ $Pb_{1.25}$ $N_{0.21}$ $O_{0.25}$ was first examined by ab initio structure determination method using the powder XRD data shown in figure 1. The initial lattice parameters were determined to be parameters and V=279.7571 $Å^3$.by an indexing procedure using the program TREOR15 in EXPO2004.16 The most probable space group was suggested to be cubic crystal system Next, the integrated intensities were extracted by the Le Bail method using the program Jana2006 (N. Tancret et al., 1996). A profile function and background function of the Le Bail method used in the present study were pseudo-Voigt function and 20thorder Legendre function, respectively. An initial structure model was then obtained by the charge flipping (CF) method17 using the extracted integrated intensities. Although the V site could not be clearly determined by the CF method using the powder XRD data, the framework structure of $Cd_{0.54}$ $La_{2.5}$ $Pb_{1.25}$ $N_{0.21}$ $O_{0.25}$ was successfully determined with the help of Rietveld refinement using JANA package shown in figure 2. Rietveld refinement of cubic crystal system having P-1 space group was found with three dimension structure as follows against XRD data shown in figure 3 for structural determination proved difficult, due to a combination of preferred orientation of the plate-like crystallites in flat-plate geometry. In other words, the extracted peak intensities for phase 1 could be reliable. Note that if the relative intensities differed a lot from the simulated patterns of the known phases, additional manual partitioning of those overlapping peaks would be necessary to get reliable intensities for the unknown multi phase 1. After considering the multiplicity and Lorentz-polarization correction, the intensities of phase 1 were used for the structure solution as below. Moreover, the reflection conditions indicated possible space group.P-1. The initial structure model was obtained using a charge flipping algorithm with the program Superflip.8 (Dan Vu et al., 2020). Random phases were used at the beginning of the charge-flipping interaction, and overlapping peaks were re-partitioned using a histogram match to improve the convergence. The iteration converged with an R factor of 29% and the final electron density shows P1 symmetry with a 5% error. The program of EDMA was then used to automatically assign atomic positions. Four unique heavy atomic positions were found and the heaviest one was assigned as Bi while the others were considered as V and Bi. Due to the existence of heavy atoms, all oxygen positions were ambiguous in the electron density map of this stage (Massiot et al., 2014). To locate the oxygen atoms, a Monte-Carlo based simulated annealing process with the program TOPAS was applied. For each annealing process,

various atomic coordinates were randomly assigned table 2 shown as the initial positions of the oxygen atoms (Lopez-Vergara et al., 2017). The annealing process was restarted after finding a few oxygen positions, until all oxygen positions were found to be reasonable with Cd ions. Overall, the crystal structure of cited crystal is octahedral closed face center cubic.

3.2. Crystal symmetry

From the analysis of the X-ray powder diffraction data collected on theMPD-PROat1000 ^{0}C, we were able to obtain good solutions from two different auto indexing programs Treor (Dubois F et al., 2001) and Dicvol implemented in X'Pert High ScorePlus. The solutions determine d by the both programs are very similar: a=14.1243 Å triclinic crystal system, with a figure of merit (FOM)M_{50} =30 and M50=65 , respectively for Treor and Dicvol [13]. From the average oxygen volume in oxides, Voxygen18–22 ˚A3 at room temperature, and the nominal composition $Cd_{0.54}$ $La_{2.5}$ $Pb_{1.25}$ $N_{0.21}$ O $_{0.25}$ we can estimate Zmax =598 /18/15=2.39 and Zmin =.11. We chose Z=2 leading to an oxygen volume slightly larger than the previous values, V oxygen =23.3 A^3. In order to determine the possible space groups of this compound, an initial procedure was performed to obtain the Bravais class. The observed intensities were extracted using a Le Bail spacegroupP-1.A Patterson function was then calculated with implement in the Full-proof suite. A strong peak was observed at 0.5, 0.5,0 leading to a triclinic Bravais class. In the whole the structure of crystal coordinated by tetrahedral geometry.

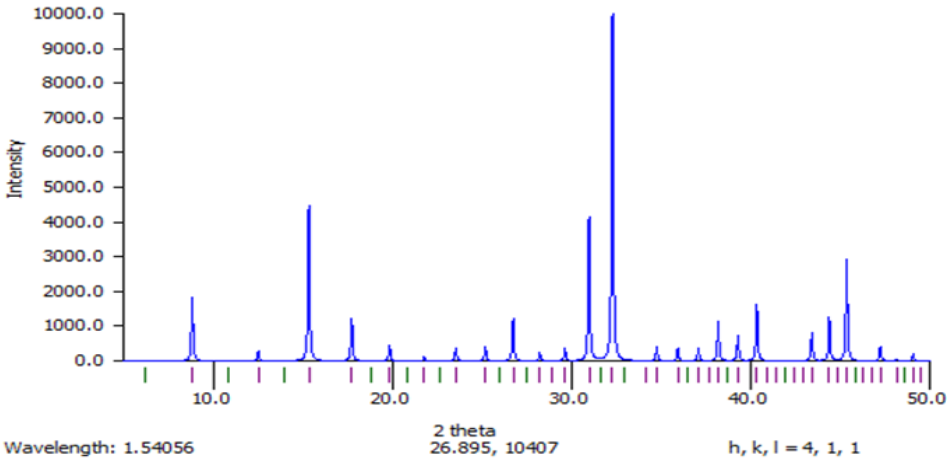

Figure 1 Powder XRD spectra of $Cd_{0.54}$ $La_{2.5}$ $Pb_{1.25}$ $N_{0.21}$ O $_{0.25}$

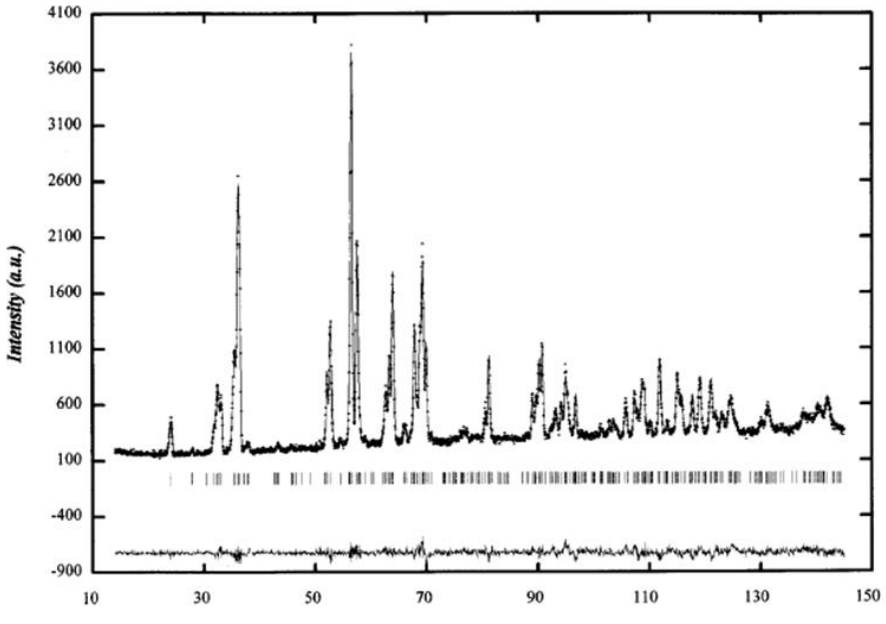

Figure 2. Graphical representation of the result from Rietveld refinement with X-ray powder data. Vertical bars indicate positions of the Bragg reflections for $Cd_{0.54}$ $La_{2.5}$ $Pb_{1.25}$ $N_{0.21}$ O $_{0.25}$ dots mark the observed intensities and the solid line gives the calculated intensity curve. The deviations between the observed and the calculated intensities from the refined model are shown by the difference plot in the lower part of the diagram.

Table1.Crystallographic Data

Phase Data		
S. N.	Properties	Data
1	Formula sum	$Cd_{0.54}\ La_{2.5}\ Pb_{1.25}\ N_{0.21}\ O_{0.25}$
2	Formula weight	673.9 g/mol
3	Crystal system	Triclinic
4	Space-group	P -1 (2)
5	Cell parameters	a=3.1346 Å b=5.3402 Å c=6.0869 Å α=79.9066° β=76.8208° γ=85.1414°
6	Cell ratio	a/b=0.5870 b/c=0.8773 c/a=1.9418
7	Cell volume	97.57 $Å^3$
8	Z	2
9	Calc. density	22.9378 g/cm^3
10	Meas.density	22.91671 g/cm^3
11	Pearson Code	aP17
12	Formula Type	N2O2P5Q8
13	Pearson code	I8d

Table2. Fraction Atomic Parameters

S. N.	Atom	Ox.	Wyck.	Site	S.O.F.	x/a	y/b	z/c	U [$Å^2$]
1	La1	+3	2i	1		0.39874	0.52349	0.26485	0.0380
2	Cd1	+2	2i	1		0.89532	0.69952	0.19451	0.0380
3	O1	-2	2i	1		0.08875	0.25861	0.49731	0.0380
4	O2	-2	2i	1		-0.09756	0.28617	0.18790	0.0380
5	O3	-2	2i	1		0.23189	0.63376	0.54389	0.0380
6	O4	-2	2i	1		0.22731	0.17865	0.17981	0.0380
7	N1	-2	2i	1		0.63272	0.00103	0.37387	0.0380
8	N2	-2	2i	1		0.93688	0.98752	0.31186	0.0380
9	N3	-2	1d	-1		1/2	1.00000	0	0.0380
10	Pb	-2	2i	1		0.50000	0.21345	0.00000	
11	Pb	-2	2i	1		0.21450	0.52143	0.45120	
12	Pb	-2	2i	1		0.32160	0.00000	0.51650	

Table3. Selected Bond Angles

S. N.	Atom1	Atom2	Atom3	Angle(^{0})
1	La1	Pb	Cd1	112.455
		Pb	O3	22.976
		Pb	Cd1	84.453
		Pb	O3	71.622
		Pb	Pb	133.323
		Pb	O2	120.684
2	Cd1	Cd1	O3	91.068
		Cd1	Cd1	116.902
		Cd1	O3	71.991
		Cd1	Pb	60.172
		Cd1	O2	71.614
		Cd1	O1	141.206
3	Pb1	Pb2	O4	134.271
		Cd1	O3	160.593
		Cd1	O1	105.024
		Cd1	O2	154.297
		Cd1	Pb	137.504
		Cd1	Pb	64.653

		Cd1	Pb	107.056
4	O1	O3	Cd1	86.547
		O3	O3	70.513
		O3	Pb	115.954
		O3	La4	123.396
		O3	O1	69.405
		O3	O4	127.043
		N1	O3	69.526
		N3	O1	31.253
		O3	O2	114.379
		O3	Pb	46.707
		O3	Pb	52.088
		N4	Pb	155.698
		Cd1	O3	155.951
		Cd1	Pb	64.892
5	Pb5	Cd1	O2	149.629
		Cd1	O1	95.734
		Cd1	O4	92.394
		O3	Pb	93.452
		O3	Pb	22.234
		O3	Pb	99.311
		Pb	O2	101.301
		Pb	O1	158.506
		Pb	O4	111.068
		Pb	O3	127.819
		Pb	O1	98.486
		Pb	Pb	121.289
6	Cd1	La1	N2	122.772
		La1	La1	116.902
		La1	Pb	62.936
		La1	O1	97.696

The heavy-atom positions M have been refined, where as the positions of the oxygen atoms have been transformed from the structural model suggested by Lundberg and Sundberg (Kanth and Mishra, 2020). Each M site was assumed in the refinement as occupied by 0.49 Cd and 0.51La. The calcium sites refined to an occupancy of 0.648(10) for Ca-1 in the 6-sided tunnels and 0.392(8) for Ca-2 inside the 7-sided tunnels. Lattice parameters for the a and b axes, determined from a calibrated X-ray diffraction pattern recorded along the [0 0 1] direction, are a =14.1243, b =14.1243, c=14.1243 Reflection intensities Ih k l were estimated using the crysfire program. Merging the intensities according to sym- symmetry yielded a data set of 556 crystallographically non-equivalent hk0 reflections after removal of 55 symmetry-forbidden reflections with non-zero intensity. The internal R-factor of symmetry-related reflections in the merged data set was 15.8% with a resolution. According to our analysis space group Pb3n was tried for solving the structure by direct methods with the program SIR97 (DO Charkin, 2008). The program was modified for this purpose with electron scattering factors provided by Jiang and Li. Similar to previous studies suspected dynamical diffraction was taken into account by using a phenomenological compensation based on The heavy Bi and V atoms, which are shown in the figure by the large grey shaded spheres, form with the oxygen atoms (small red spheres) the structural fragments of MO6 octahedral respectively. The calcium atoms are located inside the 7- (Cd-1) and 6-sided tunnels (Cd -2). The positions of the oxygen atoms have been taken from the proposed structural model of Lundberg and Sundberg and transformed to cubical space group Pn-3n.The approximation Ihklp|Vhkl| that has been derived as the limit for thick crystals under two beam conditions, where Vhkl (in volts) designates the structure factor amplitude for electrons. All attempts to use Ih k lp|Vh k l|2 instead led to wrong results with direct methods and least-squares refinement. Moreover, we found that performed geometrical corrections for parallel illumination, as suggested by other authors (G. Kresse and Joubert, 1999), spoiled the data with the result that it was neither possible to solve the structure nor to refine a given model to good geometry. Following our results obtained for the Cd0.54 La2.5 N0.21 O0.25 Pb1.25nanocrystalline powder; the data were used throughout this study without correction. The most probable solution found with these data by SIR97 had an R-factor of 40%. All 40 heavy atoms in the unit cell are clearly visible in the potential map that was calculated by the program using the 95 largest hk0 E-values. Coincidence of several additional weak peaks in the map with

suspected oxygen or cadmium atoms proved accidental and was not considered as reliable. A (kinematical) least-squares structure refinement on |Vh k l| was performed for the detected 11heavy-atom positions in the asymmetric unit (program SHELXL97-2. For the refinement, it was finally assumed that the heavy-atom positions are fully occupied by tungsten because only this yielded positive defined temperature factors for all atoms. This was not the case if mixed Nb/W sites were assumed and it is an indicator for the presence of dynamical effects. The overall R-factor of the refined framework structure was 35.2% (35] parameters refined, unit weights). The refined atomic co-ordinates together with the displacement factors Ueq are listed in Table 3. The average positional shift of the atoms during the refinement was 0.07A ˚ (maximum shift0.11 A ˚ for atom M 5). The potential map after least-squares refinement from X-ray diffraction is shown in figure1. An attempt to detect the oxygen positions from a Vobs/Vcalc difference Fourier map was unsuccessful due to the relatively high background level (lowest peak to background ratio about 3). Although several diffuse peaks appeared at the expected positions for calcium inside the 6-sided and 7-sided tunnels, the quality of the data did not allow reliable location of these atoms. Thus, the full range of available intensities up to resolution of 0.73A˚ was tested. Refinement of the heavy-metal framework with 651 unique reflections and mixed occupancies (Bi/V= 1.0) yielded an R-factor of 41.6 %. However, despite several additional peaks appeared in the Vobs-Vcalc differential Fourier map, it was again not possible without knowing the correct positions in advance to assign these peaks to the missing atoms. Since the quality of the received frame work model could not significantly be improved by the data with higher resolution, we present here only the result obtained with intensities up to 1A˚ .Nevertheless, in order to check the effect of geometrical correction on the quality of the data, we calculated the required correction factors fc which match theoretical structure factors Vh k l, calculations with uncorrected structure factors Vhkl, exp, raw and geometrical corrected structure factors Vh k l, exp precess corrected, respectively: f c = Vh k l;calc=Vh k l; exp; raw.

3.4 Crystal structure description

The crystal structure of this compound can be described by different cationic environments. Each mixed site V/Bi (1) is surrounded by eight oxygen atoms (six O (1) atoms and two O (2) atoms) at normal distances ranging from 2.47 to 2.57 with a mean distance O/Ca 2.51 A to form a slightly distorted cubical polyhedron (Figure 4). This high symmetry of the oxygen environment leads to a very weak stereo-chemical activity and the nonhybridization of the La (1) lone pair (Lp) of the atom, which is likely very close to the bismuth nucleus. The second atom Ld (2) is bounded by seven oxygen atoms to form a very distorted polyhedron, with two very short distances (2.05 and 2.09) A˚ respectively the O(3) and O(1) atoms) and normal distances varying from 2.31 to 2.49 A˚. This distorted environment is often observed when a Bi atom possesses a lone pair and the refinement of the Bi (2) electronic lone pair Lp2 places it 1.22 A from the nucleus, to occupy the interlayer between adjacent Bi (2) Ca layers. Each V-Bi (1) atom shares O(1) atoms with the six neighboring cations V-Bi(1) to form a mixed Ca-Bi-O layer parallel to the plan (b, c), associated with angles shown in table 4. In the same manner, each Bi (2) atom shares also oxygen atoms with the six closest bismuth atoms, to form a layer parallel to the precedent (Figure 4b). Thus, the crystal structure can be described by a piling of layers ABC, ABC, etc., in the a-axis direction, where layers A and C are formed by Bi(2) atoms and their oxygen environment, and layer B is constituted by mixed sites La}Bi(1) and their oxygen atoms (Figure 5). The cohesion between layers A and B is ensured by the O (1) and O (2) atoms with long distances to the Cd-La-Pb (1) atoms (Figure 4) and all bond angles are shown in Table 4.

3.5 Morphological study by SEM (scanning electron microscopy)

Scanning electron microscopy (SEM) is giving morphological examination with direct visualization. The techniques based on electron microscopy offer several advantages in morphological and sizing analysis; however, they provide limited information about the size distribution. For SEM characterization, nanoparticles solution should be first converted into a dry powder, which is then mounted on a sample holder followed by coating with a conductive metal, such as gold, using a sputter coater (Minfeng et al., 1999). The sample is then scanned with a focused fine beam of electrons. The surface characteristics of the sample are obtained from the secondary electrons emitted (Marzouki et al., 2019) from the sample surface. The morphology of the oxide nanoparticles is shown in Fig.2. From the image, it is clear that the particles were highly agglomerated in nature. The SEM pictures clearly show randomly distributed grains with smaller size. From the SEM analyses, one can conclude the formation of nanoparticles spherical structure. Here it is grown in very high-density and possessing almost uniform spherical shapes. The image reveals that the average size of the particles is 40.32 nm.

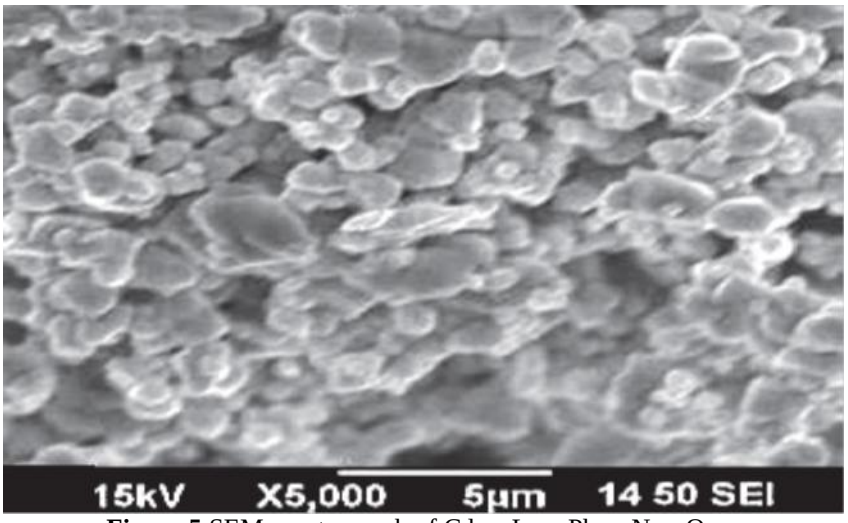

Figure 5 SEM spectrograph of $Cd_{0.54}\ La_{2.5}\ Pb_{1.25}\ N_{0.21}\ O_{0.25}$

The sample is then scanned with a focused fine beam of electrons. The surface characteristics of the sample are obtained from the secondary electrons emitted from the sample surface. The morphology of the oxide nanoparticles is shown in Fig.2. From the image, it is clear that the particles were highly agglomerated in nature. The SEM pictures clearly show randomly distributed grains with smaller size. From the SEM analyses, one can conclude the formation of nanoparticles spherical structure. Here it is grown in very high-density and possessing almost uniform spherical shapes. The image reveals that the average size of the particles is 40.32 nm.

3.6 Electrical properties

The electrical properties of the title compounds were determined by using complex impedance spectroscopy. The electrical measurements were carried out in air in the 240–360°C temperature range after stabilization at each step of 30 °C and in the frequency range 1Hz-13MHz. The applied voltage was 0.5 V, which allows eliminating aberrant points at low frequencies. Z-view computer program [19] was used to determine the electrical parameters by using a conventional electrical circuit as follow: R//CPE-R//CPE, where CPE is a constant phase element:

$$Z_{CPE} = \frac{1}{A(j\omega)^{p}} \quad \text{……..1}$$

An additional inductance L was added to account for instrumental contributions especially at high temperature. The true capacitance was calculated from the pseudo-capacitance according to the following relationships-

$$\omega_0 = (RA)^{-1/p} = (RC)^{-1} \quad \text{……2}$$

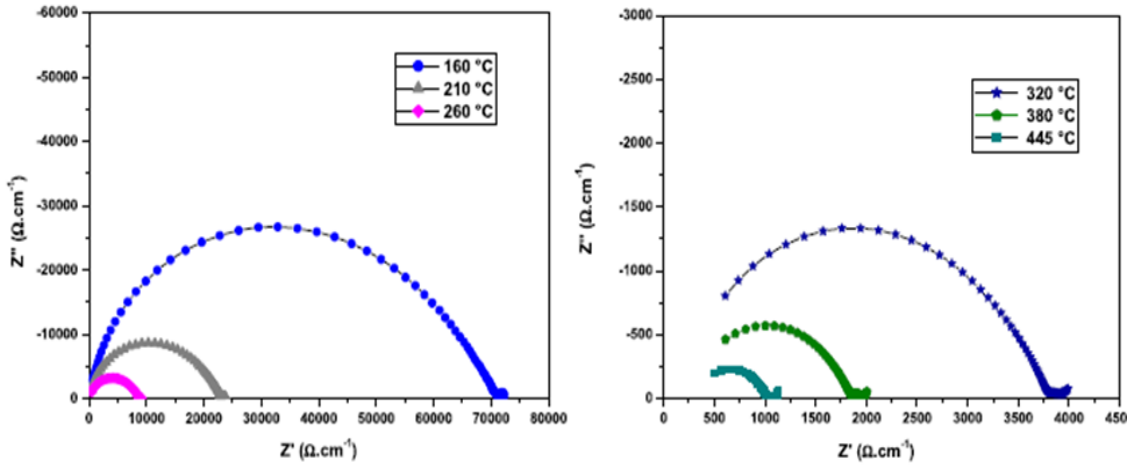

Figure6. Normalized impedance spectra recorded on $Bi_{1.25}\ V_{0.123}\ Ca_{0.245}\ N_{1.24}\ O_{8}$ at 160 °C–445 °C.

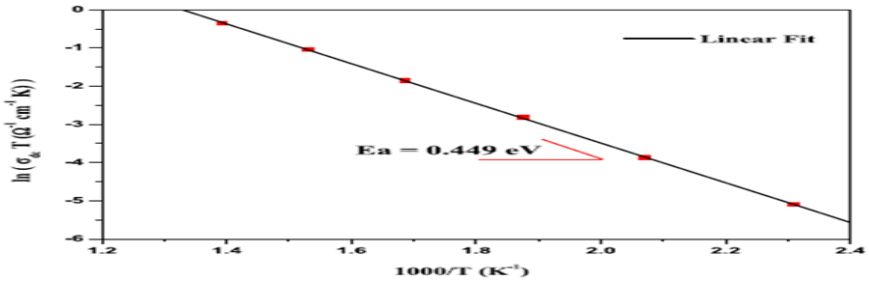

Figure 7 Arrhenius plots of conductivity of $Bi_{1.25}$ $V_{0.123}$ Ca $_{0.245}$ N $_{1.24}$ O $_{8}$.

Table4. Electrical values of the equivalent circuit parameters calculated for $Bi_{1.25}$ $V_{0.123}$ Ca $_{0.245}$ N $_{1.24}$ O $_{8}$ sample at different temperatures.

S. N.	T (℃)	T (K)	C_1(x10^{-11}F) ± 0.02	P_1 ± 0.02	ρ(k Ω. cm) ± 0.01	σ(x 10^{-4} S.cm^{-1}) ± 0.01
1	160	433	1.49	0.9	78.832	0.14
2	210	483	1.51	0.9	23.263	0.43
3	260	533	1.64	0.9	8.958	1.11
4	320	593	1.59	0.9	3.788	2.64
5	380	653	1.58	0.8	1.852	5.40
6	445	718	1.70	0.8	1.022	9.78

Normalized impedance spectra recorded on Cd0.54 La2.5 N0.21 O0.25 Pb1.25 at 150 °C–445 °Care showed in figure 6.The electrical parameters values achieved from the equivalent circuit in the temperature range 160–445°Care summarized in table 3. Where, the resistivity ρ=R/k is extracted from the refinement of each contribution which the geometric factor of the cylindrical pellet g(cm−1)=e/S (e=thickness; S=surface).The conductivity increases from 0.14 10–4 Scm^{-1} at 160 °C to 9.78 10^{-4} Scm^{-1} at 445 °C(table 3). Although, the absolute conductivity value of the Al/Li-substituted title material at 320°C (σ=2.64 10–4 Scm^{-1}). The Arrhenius plot of the electrical conductivity, log (σT) (S.Kcm^{-1})) as a function of 1000/T (K^{-1}), in the temperature interval 160 -445°C is illustrated in figure 7. As a single linear plot and following the Arrhenius law, the activation energy of the $Bi_{1.25}$ $V_{0.123}$ Ca $_{0.245}$ N $_{1.24}$ O $_{8}$compound determined by linear fit is 0.549 eV and show pseudo - order of kinetic thermal reaction. Conductivity increases with increase in temperature. This material presents interesting electrical performance and can be used as super-conductor materials [19].

IV. CONCLUSIONS

The title compound, $Cd_{0.54}$ $La_{2.5}$ $Pb_{1.25}$ $N_{0.21}$ O $_{0.25}$ has been synthesized as polycrystalline powder by solid-state method. To the present authors' knowledge, our work is the first to uncover the metal framework structure of a large unit cell heavy-metal oxide contained mixed valence with tunnel structure directly from single-projection X-ray diffraction data. To reach this goal, large-angle precession X-ray diffraction intensities have been collected on imaging plates at 100 kV. Processing of the data was performed following the quasi-kinematical approach as outlined elsewhere. Suggested data correction schemes for the geometry of off-axis hollow-cone illumination have been checked, but were not applied because this impaired the quality of the data. Thus, the framework structure of the title compound was solved from uncorrected data with 1A ˚ resolution using the direct methods program SIR97. All atoms in the asymmetric unit of the Cd0.54 La2.5 N0.21 O0.25 Pb1.25 framework were readily found by the program and correctly assigned with their 3D coordinates. A (kinematical) least-squares structure refinement of the heavy-atom positions was carried out with the program JANA using the same hk0 data set. Comparison of the refined co-ordinates for the heavy atoms resulting from Rietveld refinement on X-ray powder data (present study) showed an average agreement for the metal framework structure within 0.09A ˚ .SEM analysis of several crystallites examined indicate an average chemical composition of this phase according to Cd0.54 La2.5 N0.21 O0.25 Pb1.25 .Despite the quality of the available precession X-ray diffraction data proved sufficient for accurate determination of the heavy-atom positions, the data quality did not allow to unambiguously locate the vanadium atoms inside the tunnels nor to reveal the oxygen atoms. Theoretical calculations carried out for the M5O14 framework structure show that simple formulas for the detectability of light atoms in the presence of heavy atoms can be misleading, since the background noise which results from truncation errors in the Fourier synthesis is not taken into account. Thus, for calculated data with 1A ˚ resolution it was found that the heavy atoms appear effectively 7.8 times stronger

in the projected map than the oxygen. This explains why it would be very difficult with real data to detect the oxygen and nitrogen positions, in particular if only data from a single zone axis are considered as in the present case. The fact that it was neither possible to detect the oxygen nor the calcium atoms in the structure is a strong indicator that the data from precession X-ray diffraction still contain considerable amounts of dynamical/secondary scattering. This is also displayed by the relatively large R-factors after LS-refinement (40.2%). From our point of view, the fact that it was possible to determine the heavy-atom positions with high precision even from 100 kV data is yet a great success, because solving these types of heavy-metal framework structures directly from X-ray diffraction data was attempted by several groups for many years, but obviously, without success. Therefore, the present result is a striking example where precession X-ray diffraction reduced dynamical diffraction below the critical limit at which the determination of the structure or, at least, a fundamental part of it is enabled. However, further experiments which address to optimized conditions for detecting the oxygen atoms in heavy-atom structures seem to be necessary. So collection of 3D intensity data are likely more promising to reach this goal, since such extended data sets proved sufficient to detect even the most light atom, oxygen and nitrogen atoms. So from the above discussion we concluded that the structure of cited compound by powder pattern and the particle show nanomaterial can be used in super conductor.

Conflict of interest

There is no conflict to disclose.

REFERENCES

[1]. Bimal K. Kanth, Parashuram Mishra.(2020) Synthesis and structure determination of novel mixed valence Pb 0.5 u0.25 zr 1.25 o4.5 by powder xrd obtained from pbco3 -u(co3)2 zr(co3)2 ternary mixed valence oxides , International journal for research in applied and natural science. 6(7).

[2]. Bimal K. Kanth, Parashuram Mishra. (2020). Synthesis and Ab Initio Determination Bi1.256 La0.53 N0.231 O0.521 Zr1.543 Triclinic Structure from Powder X-Ray Diffraction Data,Sch Int J Chem Mater Sci, . 3(6): 6

[3]. DO Charkin (2008). Modular approach as applied to the description, prediction, andtargeted synthesis of bismuth oxohalides with layered structures, Russ. J. Inorg. Chem. Suppl. 53: 1977–1996.

[4]. Dubois F, Goutenoire F, Laligant Y, Suard E, Lacorre P. (2001). Ab-Initio Determination of La2Mo4O15 Crystal Structure from X-rays and Neutron Powder Diffraction. J. Solid State Chem. 2001; 159: 228−233.

[5]. G Kresse, D Joubert. (1999). from ultra soft pseudo-potentials to the projector augmented wave method, Phys. Rev. B. 59: 1758–1775.

[6]. J You, L Xin, X Yu, X Zhou, Y. Liu. (2018). Synthesis of homogenous CaMoO4 microspheres with nanopits forhigh-caapcity anode material Li-ion battery, Appl. Phys.A: Mater. Sci. Process. 124: 271-580.

[7]. Lopez-Vergara A, Porras-Vazquez JM, Infantes-Molina A, Canales -Vazquez J, Cabeza A, Losilla ER, Marero-Lopez D. (2017). Effect of Preparation Conditions on the Polymorphism and Transport Properties of La6−xMoO12−δ ($0 \le x \le 0.8$). Chem. Mater. 29: 6966−6975.

[8]. Mah Jebli, Abdessalem Badri, Mongi Ben Amara. (2019). Ab inito structure deremination Lax Bix-1Tx Journal of Chemical Crystallography.231-235.

[9]. Manickam Minakshi, David RG Mitchell, Christian Baur, B Johann Chable, Anders J Barlow, Maximilian Fichtner, Amitava Banerjee, Sudip Chakraborty, Rajeev Ahuja. (2019). Structure Determinations of Two New Ternary Oxides: Ti,PdO and Ti,Pd,O,Nanoscale Adv. 1: 565.

[10]. Minfeng Lü, Marie Colmont, Houria Kabbour, Silviu Colis, Olivier Mentré. (2014). Revised Bi/M Layered Oxo-Sulfate (M = Co, Cu): A Structural and Magnetic Study,. | Inorg. Chem. 53: 6969−6978.

[11]. N Tancret, S Obbade, N Bettahar, F Abraha. (1996). Synthesis of Ternary Metal Oxides for Battery-Supercapacitor Hybrid Devices:Influences of Metal Species on Redox Reaction and Electrical Conductivi Journal of solid state chemistry. 124: 309–318.

[12]. P Massiot, D Suard, E Goutenoire, F. (2014). La10W2O21: An Anion-Deficient Fluorite-Related Superstructure with Oxide Ion Conduction. Inorg.Chem. 53: 147−159.

[13]. Parashuram Mishra. (2011). Synthesis, crystal structure determination and ionic properties of novel BiCa0.5Mg0.5 O2.5 via X- ray powder diffraction data Crystal Growth. 20141; 2041(32): 2041-204.

[14]. Philipp Bertocco, Christoph Bolli, Bruno A. Correia Bicho, Carsten Jenne, Marc C. Nierstenhöferrate. (2019). Journal of Chemical Crystallography.

[15]. Riadh Marzouki, Youssef Ben Smida, Manel Sonni, Maxim Avdeev, Mohamed Faouzi Zid. (2019). Synthesis, structure, electrical properties and Na+ migration pathways of Na2CoP1.5As, Journal of Solid State Chemistry. 8-12,6,3.

[16]. T Dan Vu, FirasKrichen, Maud Barre, Sandrine Coste, Alain Jouanneaux,Emmanuelle Suard,Andrew Fitch, FrançoisGoutenoire. (2020). In1-xGa1+xO3(ZnO)0.5: Synthesis, structure and cation distribution, J.Solid State Chemistry, https://doi.org/10.1016/j.jssc.2020.121341

[17]. T Dan Vu,Firas Krichen, Maud Barre, Sandrine Coste, Alain Jouanneaux,Emmanuelle Suard, Andrew Fitch, François Goutenoire. (2020). Ab Initio Structure Determination of La34Mo8O75 Using Powder X-rayand Neutron Diffraction Data Cryst. Growth Des. 75-80

[18]. Thomas E Weiricha, Joaquim Portillob C, Gerhard Coxd, Hartmut Hibste, Stavros Nicolopoulosb.(2006) Ab initio determination of the framework structure of theheavy-metal oxide CsxNb2.54W2.46O14 from 100 kV precession electron diffraction data, Ultramicroscopy. 106: 164–175.

[19]. Y Liang, X Han, Z Yi, W Tang, L Zhou, J Sun, S Yang, Y Zhou. (2007). Synthesis, characterization and lithiumintercalation properties of rod-like CaMoO4 nanocrystals,J. Solid State Electrochem. , 11: 1127–1131.

[20]. Zhengyang Zhou, Lukáš Palatinus, Junliang Sun. (2019). Structure determination of modulated structures by powder X-ray diffraction and electron diffraction INORGANIC CHEMISTRY FRONTIERS. 125-128